energy&fuels

Article

pubs.acs.org/EF

Asphaltene Deposition under Dynamic Conditions in Porous Media: Theoretical and Experimental Investigation

Taraneh Jafari Behbahani,[†,‡] Cyrus Ghotbi,*[,†] Vahid Taghikhani,[†] and Abbas Shahrabadi[‡]

[†]Department of Chemical and Petroleum Engineering, Sharif University of Technology, P.O. Box 11365-9465, Tehran, Iran

[‡]Exploration and Production Division, Research Institute of Petroleum Industry (RIPI), P.O. Box 14665-1998, Tehran, Iran

ABSTRACT: In this work, a new model based on the multilayer adsorption kinetic mechanism and four material balance equations for oil, asphaltene, gas, and water phase has been developed to account for asphaltene deposition in porous media under dynamic conditions and the model was verified using experimental data obtained in this work and also with those reported in the literature. The results showed that the developed model based on multilayer adsorption kinetic mechanism can correlate more accurately the oil flooding experimental data in comparison to the previous models based on the mechanical plugging mechanism, in particular in carbonate core samples. Also, a series of experiments was carried to determine the permeability reduction of carbonate, sandstone, and dolomite core samples due to asphaltene deposition using an Iranian bottom hole live oil sample which is close to reservoir conditions in order to study the effect of different parameters on asphaltene deposition mechanisms during dynamic conditions in porous media. The performance of the effective parameters of porous media on asphaltene deposition such as mineral composition and morphology of surface was also studied using X-ray, elemental analysis, and scanning electron micrographs (SEMs). It was found that an increase of the iron content of core sample leads to a less permeability damage and an increase of the calcium content of core sample leads to an increase of the permeability damage during natural depletion due to asphaltene deposition. SEMs of carbonate core sample showed the formation of large clusters of asphaltene with characteristic sizes that greatly exceed the monolayer deposition characteristic size. Also, a novel experimental method was designed and proposed to distinguish between the mechanical plugging and adsorption mechanisms of asphaltene using the cyclohexane or toluene reverse flooding and it has been found that 60−82% permeability reduction by asphaltene deposition was caused by mechanical plugging mechanism during a fast process, whereas 18−40% of formation damage is due to an adsorption mechanism that takes place in a longer time.

1. INTRODUCTION

Asphaltenes and resins are the polar fractions of crude oil that can be separated by addition of low molecular weight *n*-alkanes. By definition, asphaltenes are the fraction of a crude oil that is soluble in toluene and insoluble in an *n*-alkane, typically pentane or heptane. These fractions are formed by molecules with a polyaromatic structure containing paraffinic and naphthenic chains, as well as oxygen, nitrogen and sulfur as functional groups or heteroatom. In the other hand, asphaltenes are heavy hydrocarbon molecules that are stabilized by resins adsorbed on their surface in the oil.[1] Asphaltenes can reduce the hydrocarbon effective mobility by

- Blocking pore throats thus reducing the rock permeability.
- Adsorbing on to the rock and altering the formation wettability from water-wet to oil-wet, therefore decreasing the effective permeability to oil and increasing the irreducible oil saturation.
- Increasing the reservoir fluid viscosity.

The processes of asphaltene precipitation and deposition in porous media have a substantial effect on oil flow during primary oil production and enhanced oil recovery processes. The oil flows through regions with the minor resistance during primary production stage of a reservoir. The natural depletion of a reservoir may cause the precipitation and flocculation of asphaltenes decreasing the productivity of a well during primary oil recovery. Due to the complexity of asphaltene deposition phenomena during production, very little experimental results currently exist on asphaltene deposition under dynamic conditions using bottom hole live oil in porous media. The majority of existing works study the asphaltene deposition during core flooding using the injection of recombined oil (mixture dead oil and associated gas) to the core and or with static systems and in the absence of a reservoir rocks.[2−5]Therefore, such results are not applicable to the real scale, where the flow as well as complex interactions between the fluid and the porous medium are always present. The asphaltene deposition is governed by four mechanisms; surface deposition, entrainment, plugging, and adsorption. Ali and Islam[6] investigated the effect of asphaltene deposition on carbonate rock permeability in single-phase flow. Gruesbeck and Collins[7] proposed a model that has been used for mechanical entrapment of solids and developed the equation for the deposition of fines in porous media. Minssieux et al.[8] investigated the flow properties of crude oils at reservoir temperature in different rocks. Leontaritis[9] developed a simplified model for prediction of formation damage and productivity decline by asphaltene deposition under saturated conditions in radial flow. The hydraulic diameter was estimated by the ratio of the total pore volume to the total pore surface area of the flow channels. Civan[10] developed a two-phase

Received: August 8, 2012
Revised: January 7, 2013
Published: January 9, 2013

   dx.doi.org/10.1021/ef3017255 | *Energy Fuels* 2013, 27, 622−639

model to predict paraffin and asphaltene deposition. The permeability of plugging and nonplugging pathways was given by empirical relationships. Wang et al.[11] proposed a deposition model including the static and dynamic pore surface deposition and pore throat plugging. Nghiem et al.[12] proposed a model to study compositional simulation of asphaltene precipitation. They used the developed equation of Kumar and Todd[13] based on the Kozeny−Carman equation. Kocabas et al.[14] developed a wellbore model coupled to asphaltene adsorption model based on the Langmuir equation for linear and radial systems. The model proposed by Ali and Islam was used, and the equation was solved analytically through Laplace transform. Wang and Civan[15] proposed a model which the asphaltene mass balance equation is incorporated into a three-dimensional, three-phase black oil simulator .The deposition rate for asphaltene includes three terms: the surface deposition, the entrainment, and the pore throat plugging rate. Almehaideb[16] developed a model to simulate asphaltene precipitation, deposition, and plugging of oil wells during primary production. The model was implemented in cylindrical coordination to match the flow direction around the well. Monteagudo et al.[17] used network modeling to simulate one-phase flow in porous media in order to predict the change in petroleum flow by asphaltene deposition. The adsorption of asphaltenes on solids is the result of favorable interactions of the asphaltene species or its aggregates with chemical species on or near the mineral surface. A number interaction forces, individually or in combination with each other, can be responsible for it. The major forces that can contribute to the adsorption process include electrostatic (Coulombic) interactions, charge transfer interactions, Van der waals interactions, repulsion or steric interactions, and hydrogen bonding.[18−20] Soulgani[21] developed a new expression for the surface deposition term and implemented in asphaltene deposition modeling. Lawal[22] developed a new asphaltene deposition model by incorporating kinetics of asphaltene deposition under dynamic conditions in to the deep-bed filtration theory.

In this work, a new model for asphaltene deposition based on multilayer adsorption kinetic mechanism and four material balance equations (oil, asphaltene, gas, and water phase) in porous media during dynamic condition was developed and the model was verified using experimental data obtained in this work and also found in the literature. In the Experimental Section using bottom hole live oil sample which is close to reservoir conditions, the influence of effective parameters on asphaltene deposition mechanisms such as composition and morphology of porous media were investigated. Also, a novel experimental method was designed and proposed to measure the amount of deposited asphaltene due to different mechanisms using the cyclohexane or toluene reverse flooding.

2. EXPERIMENTAL SECTION

2.1. Materials. In the majority of previous works, the mixture of recombined oil (mixture dead oil and associated gas) was injected in core sample which is far from reservoir conditions. In this work, a bottom hole live oil sample from an Iranian reservoir in the Southeast region of Iran which is close to reservoir conditions was used. The specific gravity and viscosity of the bottom hole live oil sample were measured to be 0.9322 and 4.35 cP at the reservoir pressure, respectively. The compositional analysis of crude oil was performed and given in Table 1. The results were obtained using the gas chromatography method.[23] The formation water sample was collected from the same oilfield, cleaned, and analyzed. The details of physical and chemical properties were listed in Table 2. Various carbonate, dolomite, and sandstone cores having cylindrical shape with lengths ranging from 4 to 30 cm and constant diameter equal to 4 cm were extracted at various depths of the Iranian wells and, then, characterized and tested in the EOR Research Center laboratory, Research Institute Petroleum of Industry (RIPI). The investigated core samples were cleaned prior their use, by using various solvents (Soxhlet extraction with xylene, methanol, and chloroform) according to the ASTM D2172 procedure.[24] Their characteristics including their porosities, permeabilities, and pore volumes were shown in Table 3. It should be noted that the core sample no. 1 was extracted from the studied oil reservoir. As listed in Table 3, the measured porosities were in the range of φ = 12.6−26% and the measured absolute permeabilities were in the range of k = 1.4−106.6 mD. Also, the X-ray diffraction (XRD) measurements were carried out to study the structure of core samples by the Philips PW 1820 diffractometer (Cu Kα, λ = 0.154 nm). Table 4 shows the mineralogy data obtained from the X-ray analysis.

The asphaltene content of the bottom hole live oil was measured to be wasp = 16.3 wt % using the SARA analyses .The constituents of crude oils are typically classified by solubility saturates aromatics, resins, and asphaltenes (SARA). For SARA fraction analysis, asphaltene fraction was extracted from crude oil by precipitation with *n*-heptane as described by the ASTM D3279-97 procedure.[25] Subsequent elution with a series of increasingly polar solvents as the mobile phase yields saturates (eluted with a nonpolar solvent such as hexane), followed by the elution of aromatics with toluene, and finally by the elution of resins with a more polar solvent. The SARA analyses results of bottom hole live oil are shown in Table 5. To determine the PVT and phase behavior of the bottom hole live oil, various experiments were conducted (DBR, VINCI PVT Cell). In Table 6, the PVT characteristics and phase behavior of the studied bottom hole live oil

Table 1. Studied Bottom Hole Live Oil Compositions

components	bottom hole live oil (mol %)	components	bottom hole live oil (mol %)
H_2S	0	*n*-C5	1.59
N_2	0.3	C6	6.95
CO_2	1.83	C7	4.1
C1	22.7	C8	3.88
C2	8.24	C9	2.49
C3	6.14	C10	4.03
i-C4	1.19	C11	2.85
n-C4	3.61	C12+	28.74
i-C5	1.38	total	100

Table 2. Physical and Chemical Properties of Formation Water Sample

property	value
viscosity (CST @ 40 °C)	0.9166
pH at 20 °C	6.5
oil (mg/L)	4
chemical oxygen demand (mg/L)	1216
biological oxygen demand (mg/L)	530
total suspended solids (mg/L)	352
chloride (mg/L)	123100
$CaCO_3$ (mg/L)	177
sulfate (mg/L)	291
total dissolved solids (mg/L)	202050
potassium (g/L)	1.1
sodium (g/L)	60
calcium (mg/L)	13280
magnesium (mg/L)	1262
iron (mg/L)	42
strontium (g/L)	0.58
lithium (mg/L)	13
sulfide (mg/L)	7.2
barium (mg/L)	1.2

dx.doi.org/10.1021/ef3017255 | Energy Fuels 2013, 27, 622−639

Table 3. Characteristics of the Various Studied Core Samples

sample no.	type of core	length (cm)	diameter (cm)	porosity (%)	permeability (mD)	grain density (g/cm^3)	weight (g)	PV
1	carbonate	4.5	3.7	26	2.7		103.8	13.5
2	dolomite	5.1	3.8	22.5	106.6	2.68	118.5	12.3
3	sandstone	5.96	3.7	13.15	22.8	2.65	150.8	8.5
4	sandstone	30	3.8	12.6	1.4		548	28.8

Table 4. X-ray Analysis of the Various Studied Cores

	composition			
sample no.	1	2	3	4
SiO_2	0.79	22.97	56.3	62.4
Al_2O_3	0.16	3.29	9.06	8.12
SO_3	0.56	0.23	0.23	0.12
Fe_2O_3	0.1	1.34	2.67	3.65
Na_2O	0.18	0.9	2.29	2.21
K_2O		0.54	1.76	2.45
CaO	54.6	37.35	12.95	8.52
MgO	0.38	3.07	1.59	1.25
MnO			0.12	0.18
TiO_2		0.23	0.36	0.48
Cl	0.16	0.48	0.19	0.15
LOI	43.02	29.5	12.38	10.47

Table 5. SARA Test Results of the Studied Bottom Hole Live Oil

type of group	bottom hole live oil
saturate (wt %)	32.61
aromatic (wt %)	43.48
resin (wt %)	7.61
asphaltene (wt %)	16.3

Table 6. *PVT* Characteristics and Phase Behavior of the Studied Bottom Hole Live Oil

reservoir pressure, P_{res} (bar)	326
reservoir temperature, T_{res} (°C)	96
molar weight of the bottom hole live oil (g/mol)	182
saturation pressure, P_{sat} (bar)	97
specific gravity of bottom hole live oil	0.9322
molar weight of the heavy group (bottom hole live oil), C12+ (g/mol)	491
specific gravity of the C12+ fraction	0.9853
molar weight of the heavy group (dead residual oil), C12+ (g/mol)	395
GOR (SCF/STB)	305
upper onset pressure at reservoir temperature (bar)	276
lower onset pressure at reservoir temperature (bar)	38

are shown. Also, solution gas−oil ratio (GOR) and oil formation volume factor versus pressure are shown in Figures 1 and 2.

Figure 1 shows that variation of the solution GOR was from 0 to 360. Also, variation of oil formation volume was from 1.05 to 1.3 as shown in Figure 2.

2.2. Experimental Apparatus. Figure 3 shows the schematic of the experimental setup used in this work in order to determine the effect of asphaltene deposition on the properties of a reservoir rock samples. This setup consists mainly of the following devices:

- An automatic displacement pump (Vinci, p = 10 000 psi, accuracy = 0.1 psi) was used to displace the crude oil, reservoir formation water through the composite reservoir core plug inside a core holder (Temco).
- Four high pressure stainless steel cylinders (500-10-P-316-2, DBR, Canada) were used to store and to deliver the bottom

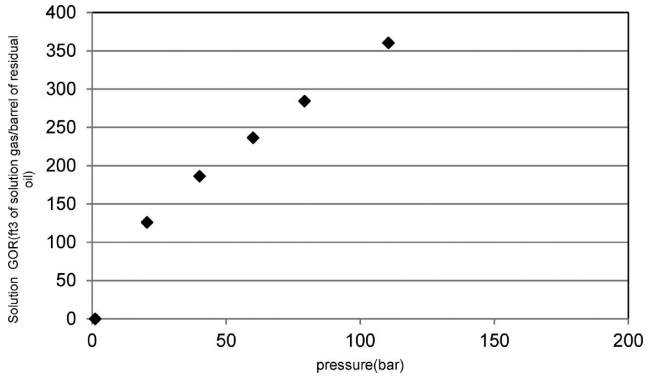

Figure 1. GOR results for the studied bottom hole live oil.

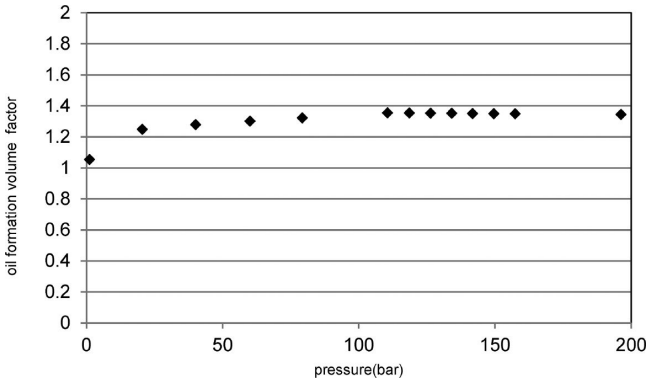

Figure 2. Variation of oil formation volume factor versus pressure for the studied bottom hole live oil.

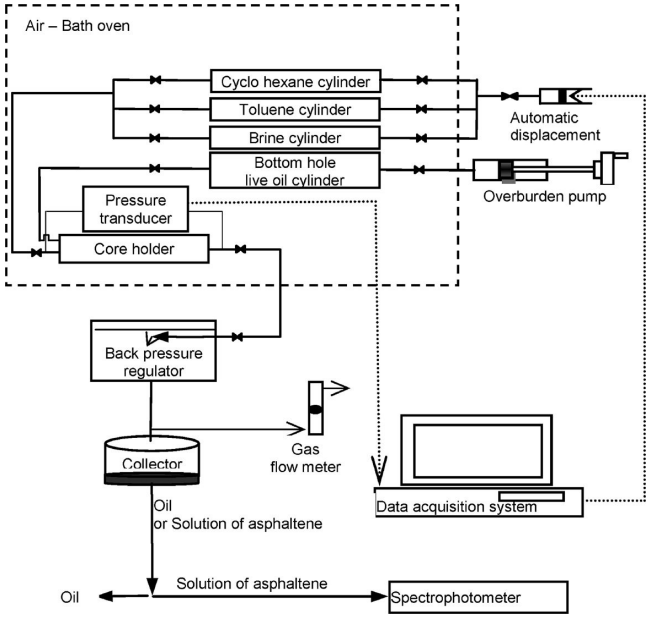

Figure 3. Schematic of experimental setup.

dx.doi.org/10.1021/ef3017255 | *Energy Fuels* 2013, 27, 622−639

Table 7. Experimental Conditions and Oil Permeability Reduction Data for Oil Flooding Tests

					oil permeability reduction (%)		
test no.	core sample	S_{Wc}	S_{Oi}	Q (cm^3/h)	total	due to mechanical plugging mechanism	due to adsorption mechanism
IRS1	3	36.7	63.3	1	76.2	62.5	13.5
IRS2	3	36.7	63.3	3	78.5	62.8	15.2
IRS3	3	36.7	63.3	10	79.4	62.7	16.5
IRS4	3	36.7	63.3	30	81.5	66.3	15.1
IRS5	4	37	63	10	84.6	67.68	16.92
IRC1	1	43.7	56.3	1	63.5	38.1	25.4
IRC2	1	43.7	56.3	5	78.1	61	24.1
IRC3	1	43.7	56.3	10	81.4	65.12	16.28
IRD1	2	43.7	56.3	3	65.4	40.5	26.1
IRD2	2	43.7	56.3	5	71.2	56.96	14.24

Table 8. Experimental Results of Formation Damage by Mechanical Plugging and Adsorption Mechanisms

	deposited asphaltene (mg/m^2)	
test no.	mechanical plugging mechanism	adsorption mechanism
IRS1	4.53	
		4.15
R.SD (%)	1.2	0.98
IRS2	5.52	
		3.51
R.SD (%)	0.88	0.98
IRS3	4.25	
		2.97
R.SD (%)	0.65	0.88
IRS4	5.43	
		4.32
R.SD (%)	1.4	0.82
IRS5	6.54	
	---	4.56
R.SD (%)	1.2	1.1
IRC1	8.54	---
	---	6.72
R.SD (%)	1.1	1.0
IRC2	8.76	---
	---	5.95
R.SD (%)	0.95	0.86
IRC3	9.15	---
	---	6.54
R.SD (%)	1.3	0.93

hole live oil sample and reservoir formation water, cyclohexane, and toluene (DBR, capacity of 500 mL).

- The core holder (Temco, p = 10 000 psi, T = 150 °C), horizontally placed, held a core through a sleeve. A constant overburden pressure was applied around this sleeve, which was always kept 5 MPa higher than the inlet pressure of the core holder. The inlet and outlet ports of the core holder were connected to the pressure transducer. The inlet ports of the core holder were also connected to the positive displacement pump. Four cylinders containing reservoir formation water, bottom hole live oil sample, cyclohexane, and toluene allowed injection of sample inside the core holder. The positive displacement pump was operated at constant rate or in pressure mode. The pressure drop during the core flood tests was measured with a digital pressure indicator. The core flooding system was thermoregulated by means of an air bath oven. An important feature was the possibility for continuous measurement of the pressure drop along section of the porous medium. The annular space between the sleeve and the body was filled with paraffin oil which the confining pressure was applied on the external surface of the sleeve.
- A pressure transducer (Jumo, accuracy = 0.05) was used to accurately record the pressure data.
- A back-pressure regulator (Jeafer DBR, p = 10 000 psi, T = 250 °C) was used to maintain the prespecified injection pressure inside the core holder during each flooding test.
- An overburden pump (Enerpac, p = 10 000 psi).
- An air-bath oven (Vinci, T = 200 °C).
- Rigid valves.
- A data acquisition system (Logger screen 500 Jumo: pressure, temperature, volume).
- A double-beam UV−vis spectrophotometer (Cary 4000, Varian, Inc.) was used to measure the amount of deposited asphaltene in core plug samples. The spectrophotometer used in this study was slightly modified to accommodate a quartz flow cell (Starna Cells, Inc.) with a 4 mL nominal volume and 10 mm path length in the sample compartment. To calibrate the spectrophotometer for each sample, a cyclohexane and or toluene solution including asphaltene with a concentration of 500 mg/L was prepared and diluted for making lower concentration solutions. Then, absorbance of each solution was measured in the 100−700 nm range. Also, those asphaltene particles that pass the core sample without being trapped or adsorbed has been measured as asphaltene content of outlet oil flow using a SARA test.

2.3. Experimental Procedure. Various sets of experiments were conducted with different objectives regarding to asphaltene deposition. In each experiment, first, the core plugs were dried and vacuumed at 0.7 bar for 1 h. Then, the formation water was imbibed to measure the pore volume of the reservoir core plugs. Afterward, the formation water was injected at different rates (1−30 cm^3/h) to determine water permeability of the core plugs. Then, the formation water was displaced by the bottom hole live oil until reaching the irreducible water saturation.

The initial connate water saturation was found to be 36.7−43.7%, and the initial oil saturation was in the range of 56.3−63.3% for the core samples. After the core plugs were fully saturated with the oil, the live oil was injected to the core plugs and several flooding tests were conducted. The differential pressure (ΔP) between the inlet and outlet of the core holder was measured by a digital pressure indicator and was indicated by the data acquisition system at a preset time interval. The onset pressures of the studied bottom hole live oil (upper onset pressure and lower onset pressure at reservoir temperature) are given in Table 6. It should be noted that pressure injection is above onset pressure in all experiments. As regards the back pressure is 18 MPa and pressure drops measured are above 7 MPa; therefore, the injection pressure is above onset pressure in all experiments. Also, it should be mentioned that the experiments were conducted out at specified flow rate as shown in Table 7 in each test.

Tests given in Table 7 were conducted to determine the oil permeability reduction due to different asphaltene deposition mechanisms induced by natural depletion in the core samples. Natural depletion

dx.doi.org/10.1021/ef3017255 | Energy Fuels 2013, 27, 622−639

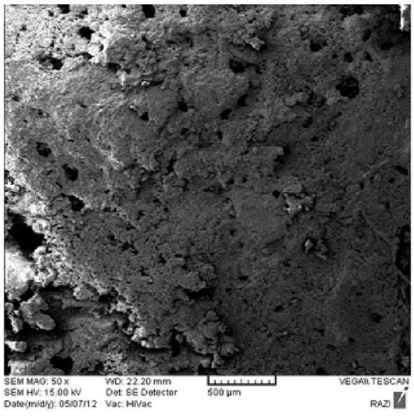

a) The carbonate core sample before flooding

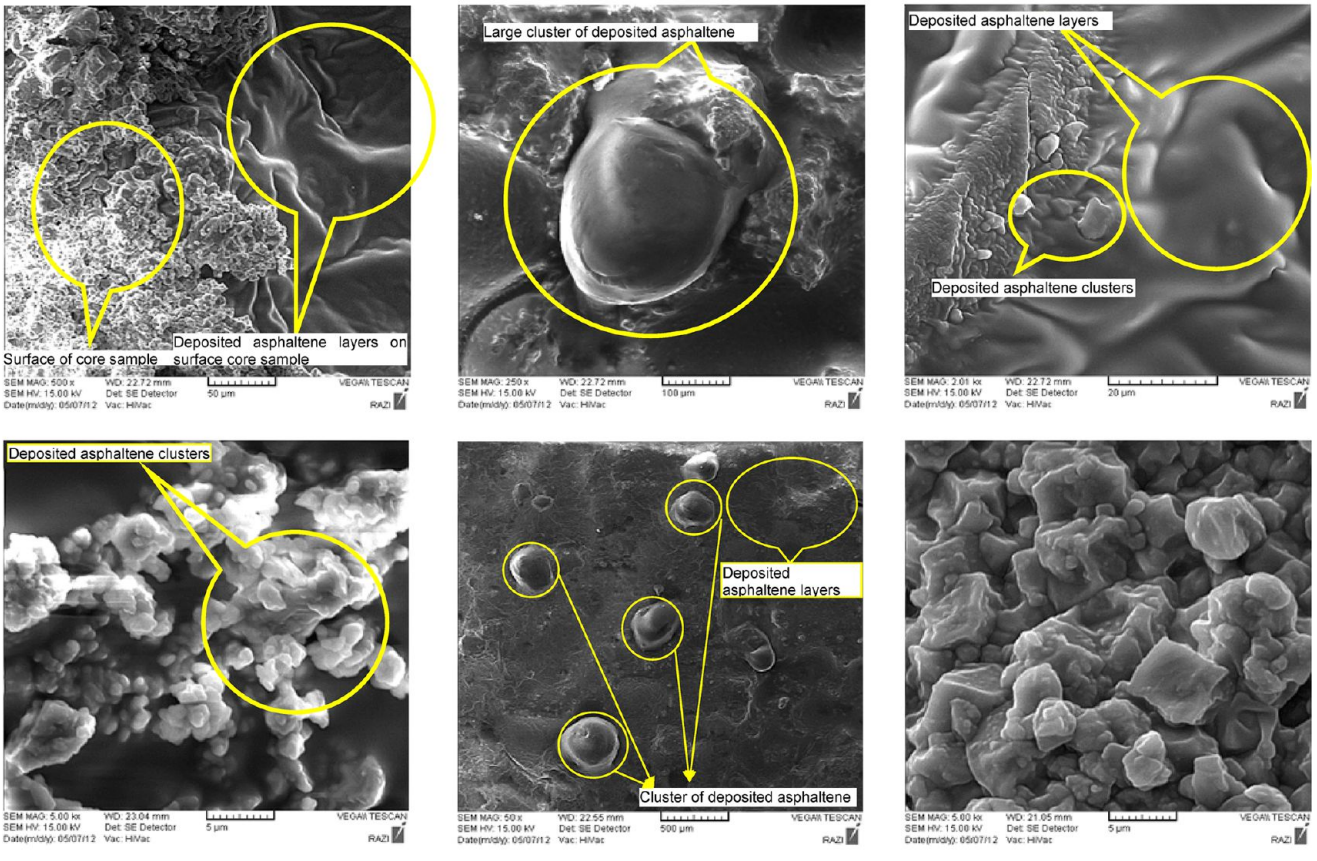

b) The carbonate core sample after flooding

Figure 4. SEM images of studied carbonate core sample.

was performed at different flow rates, 1−30 cm^3/h, and at a constant temperature of 96 °C. In each test, the injection was continued to reach a stable differential pressure and no more oil was produced.

2.4. Novel Experimental Proposed Procedure in Order to Distinguish between the Mechanical Plugging and Adsorption Mechanisms during Asphaltene Deposition. Test nos. 1, 3, 5, 7, 9, 11, 13, 15, 17, and 19 given in Table 8 were designed to measure the permeability reduction and the amount of deposited asphaltene during natural depletion and recovery of formation damage due to mechanical plugging mechanism. The spectrophotometer was used for measuring concentration of deposited asphaltene due to two mechanism, plugging and adsorption. It should be noted that the oil flooding experiment was performed in the first step and then cyclohexane and toluene flooding experiments were performed, respectively. Therefore cyclohexane and toluene flooding removed deposited asphaltene in the first step. Those asphaltene particles that pass the core sample without being trapped or adsorbed has been measured as asphaltene content of outlet oil flow.

It should be noted due to neutrality of cyclohexane on asphaltene dissolving, cyclohexane reversal flooding removes the deposited asphaltene on the surface due to mechanical trapping mechanism and due to reaction of toluene with adsorbed asphaltene on active sites of core sample, and toluene reverse flooding removes the adsorbed asphaltene by adsorption mechanism. The measured concentration of asphaltene in cyclohexane or in toluene by spectrophotometer shows deposited asphaltene due to each mechanism, plugging, or adsorption. Novel experimental proposed procedure was explained as follow.

Step 1: In first step, oil flooding experiments were conducted in the core sample. These experiments consisted of natural depletion to deposit asphaltene on core sample. Those asphaltene particles that pass the core sample without being trapped or adsorbed have been measured as asphaltene content of the outlet oil flow.

dx.doi.org/10.1021/ef3017255 | *Energy Fuels* 2013, 27, 622−639

Step 2: In order to measure and to restore formation damage due to mechanical plugging mechanism, cyclohexane reverse flooding at a flow rate of 30 cm^3/h was performed. In each test, the cyclohexane injection was continued until a stable differential pressure reaches and the permeability recovery factors were determined. It should be noted that cyclohexane reverse flooding removed deposited asphaltene due to mechanical plugging in core sample at first step.

Step 3: The asphaltene concentration of cyclohexane solution obtained in step 2 was measured using a double-beam UV−vis spectrophotometer as the amount of deposited asphaltene in core plug due to mechanical plugging mechanism.

Step 4; Then, the oil flooding was performed to measure the oil permeability reduction due to mechanical plugging mechanism.

Step 5: Test nos. 2, 4, 6, 8, 10, 12, 14, 16, 18, and 20 given in Table 8 were proposed to measure the permeability reduction and the amount of deposited asphaltene during natural depletion and recovery of formation damage due to adsorption mechanism of asphaltene. For this purpose, after the mechanical damage removal experiment, the reverse flooding of the core with toluene was followed. Toluene is the dissolving agent of adsorbed asphaltenes that cannot be removed with the cyclohexane reverse flooding in previous tests. In each experiment, permeability recovery factors were determined.

Step 6: Finally, asphaltene content of toluene solution obtained from toluene reverse flooding process was measured using UV−vis spectrophotometer as the amount of adsorbed asphaltene in the core plug due to adsorption mechanism.

Step 7: Then, the oil flooding was performed to measure the oil permeability reduction due to asphaltene adsorption mechanism.

2.5. SEM and EDX Analysis. Scanning electron microscopy was used to analyze the morphology and structure of core samples using a VEGA, TESCAN SEM in the Razi Metallurgical Research Center. Four core samples from Iranian formations were examined before and after flooding. A thin section of the core samples was cut at a thickness of 1 cm. One piece of each sample was dried and placed on a sample holder, and after flooding, a thin gold layer was applied under vacuum condition to improve signals and to reduce charging on surface. The SEM can reveal topographic details of a surface with great clarity and detail. High quality images on a micrometer scale can be obtained using SEM analysis. It can resolve morphologic details of less than 5 μm and possesses a depth of focus more than 500 times higher than that of the optical microscope at equivalent magnifications. These images are created by focusing a high-energy beam of electrons onto the sample and detecting interactions that occur at the sample surface.

Also, the elemental analysis of all core samples were determined with targeted compositions by inductively coupled plasma mass spectrometry (ICP-MS) and energy disspersive X-ray (EDX) analysis which is an integrated feature of the scanning electron microscope operating at 25 kV.

3. DEVELOPED MODEL FORMULATION

Due to the adsorption and mechanical trapping mechanisms, asphaltenes can change morphology and wettability of reservoir rock which in turn cause a modification in oil flow. The asphaltene adsorption on core surface is a major responsible of wettability alteration of formations. In all the previous models the asphaltene deposition is based on the Gruesbeck and Collins experiments[7] for fine mineral particles which is based on only mechanical trapping mechanism, and it is different from the asphaltene adsorption mechanism. A recent study by AlAwadhy[26] shows that no change in permeability during oil flooding is observed when the same crude oil is deasphalted before flooding. The asphaltenes adsorption mechanism, which is related to the interactions between the asphaltenes functional groups and the rock surface, involves surface polarity, affinity, or other attractive forces. Asphaltene is a positive polar component; therefore, formations especially carbonate core sample have the ability to adsorb asphaltene as multilayer.

The SEM analysis of asphaltene adsorption on core samples, in this work, shows the formation of asphaltene adsorption as a multilayer with characteristic sizes that greatly exceeds the monolayer adsorption size especially on carbonate core sample as shown in Figures 4−6. Therefore, the asphaltene deposition modeling is not only according to mechanical plugging mechanism but also is according to asphaltene adsorption mechanism as a multilayer. Therefore, based on experimental analysis in this work, the asphaltene adsorption model has been developed around a multilayer mechanism of adsorption as follows.

3.1. Developing Multilayer Kinetic Adsorption Model for Asphaltene Adsorption during Dynamic Condition on Porous Media. In this model two steps are considered for asphaltene adsorption. The first adsorption step is taken as adsorption of asphaltenes in solution to the surface of the rock and the second adsorption step is taken as the adsorption of asphaltenes in solution to those asphaltenes already adsorbed to the rock.

On the basis of the multilayer adsorption theory,[27] the multilayer kinetic adsorption model was defined as follows:

$$\frac{\partial \Gamma}{\partial t} = \Gamma_\infty k_1 (Cn^{-1} + k_2 C^n) - \Gamma[k_1 C(1 + k_2 C^{n-1}) + 1] \tag{1}$$

Also, the multilayer adsorption equilibrium model[27] gives the following relation for the amount of adsorbed asphaltene (Γ):

$$\Gamma = \frac{\Gamma_\infty k_1 Cn^{-1} + \Gamma_\infty k_1 k_2 C^n}{1 + k_1 C + k_1 k_2 C^n} \tag{2}$$

3.2. Modifying the Equation of Asphaltene Flow Rate through Porous Media. Asphaltene flow rate through porous media is governed by the convection−dispersion−adsorption transport equation, which in one dimension has the form:

$$D\frac{\partial^2 c}{\partial x^2} - v\frac{\partial c}{\partial x} = \frac{\partial c}{\partial t} + \rho_A \frac{\partial E_A}{\partial t} \tag{3}$$

The first term of eq 3 represents the dispersion, whereas the second term represents convection. The first term of the right side represents accumulation, and the last term represents asphaltene deposition as well as mechanical plugging rate.

In this work, equation of asphaltene flow rate through porous media, eq 3, was modified by including new multilayer kinetic adsorption term, eq 1, to asphaltene deposition rate as follow:

$$D\frac{\partial^2 c}{\partial x^2} - v\frac{\partial c}{\partial x} = \frac{\partial c}{\partial t} + \rho_r \frac{(1 - \emptyset)}{\emptyset}\left(\frac{\partial E_A}{\partial t} + \frac{\partial \Gamma}{\partial t}\right) \tag{4}$$

Hence, equation of asphaltene flow rate through porous media has been modified as follows:

$$D\frac{\partial^2 c}{\partial x^2} - v\frac{\partial c}{\partial x} = \frac{\partial c}{\partial t} + \rho_r \frac{(1 - \emptyset)}{\emptyset}\left[\Gamma_\infty k_1 (Cn^{-1} + k_2 C^n) - \Gamma[k_1 C(1 + k_2 C^{n-1}) + 1] + \frac{\partial E_A}{\partial t}\right] \tag{5}$$

3.3. Asphaltene Deposition Model. The mechanical plugging rate for asphaltene is given according to Wang model[15] based on the work of Gruesbeck and Collins[5] as follows:

$$\partial E_A/\partial t = \alpha S_L C\phi - \beta E_A(v_L - v_c) + \gamma S_L u_L C \tag{6}$$

dx.doi.org/10.1021/ef3017255 | Energy Fuels 2013, 27, 622−639

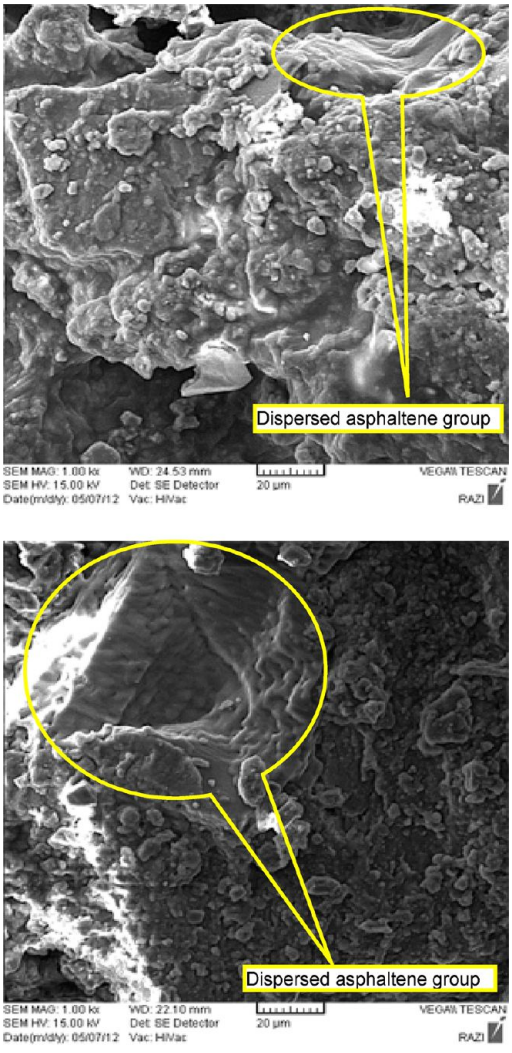

Figure 5. SEM image of studied sandstone core samples after oil flooding.

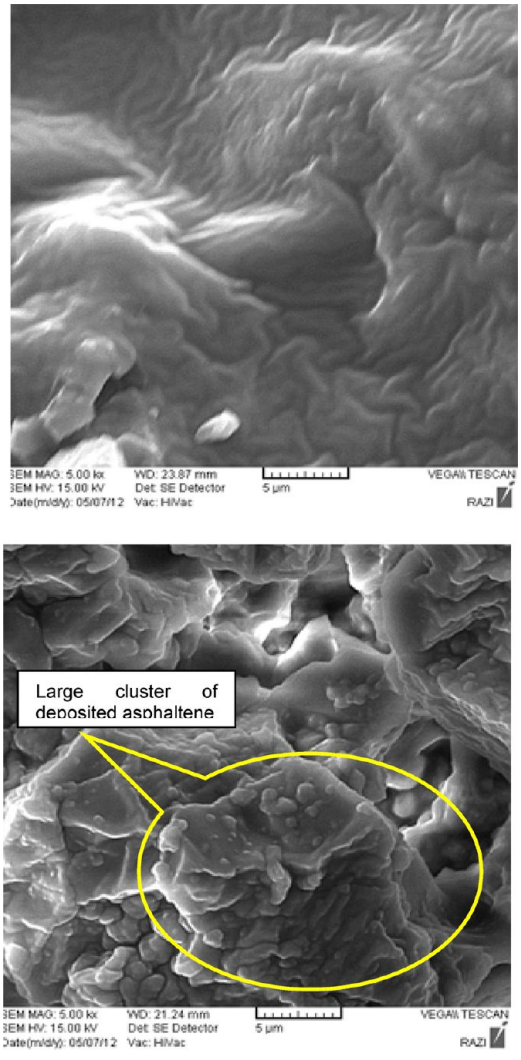

Figure 6. SEM image of studied dolomite core sample after oil flooding.

where the first term represents the surface deposition rate. The second term represents the entrainment of deposited asphaltene by the flowing phase when the interstitial velocity is larger than a critical interstitial velocity. This term shows that the entrainment rate of the asphaltene deposition is directly proportional to the amount of asphaltene deposits present in porous media, and also, the difference between the actual interstitial velocity and the critical interstitial velocity necessary for deposited asphaltene mobilization. The last term indicates the pore throat plugging rate, which is directly proportional to the product of the superficial velocity and the asphaltene precipitate concentration in the liquid phase. The value of β is described as

$$\beta = \beta_i, \quad \text{when } v_L > v_c$$
$$\beta = 0, \quad \text{otherwise}$$
$$v_L = \frac{u_L}{\emptyset} \tag{7}$$

The value of γ is set as

$$\gamma = \gamma_i(1 + \sigma E_A), \quad \text{when } D_{pt} < D_{ptcr}$$
$$\gamma = 0, \quad \text{otherwise} \tag{8}$$

Thus, the pore throat plugging deposition rate increases proportionally with the total deposits. When D_{pt} is less than D_{ptcr}, pore throat plugging deposition will occur.

3.4. Mass Balance Models. It should be noted that the asphaltene deposition modeling are represented by mass balance models for the liquid and asphaltene, the momentum balance equation, the asphaltene precipitation and deposition relations, and the porosity and permeability reduction equations. The majority previous works use two material balance based on oil and asphaltene equations phase for core samples. The proposed model in this work is an extension of the traditional black oil equations described by Wang and Civan.[15] The material balance equations are included for the water and gas component during flooding processes and therefore the material balance equations are proposed as follows:

Oil phase

$$\frac{\partial}{\partial t}(\phi S_L \rho_L w_{OL}) + \frac{\partial}{\partial x}(\rho_L u_L w_{OL}) = 0 \tag{9}$$

Gas phase: light component s present in vapor and liquid phases

$$\frac{\partial}{\partial t}(\phi S_V \rho_G + \phi S_L \rho_L w_G) + \frac{\partial}{\partial x}(\rho_L u_L w_G + \rho_L u_G) = 0 \tag{10}$$

dx.doi.org/10.1021/ef3017255 | Energy Fuels 2013, 27, 622−639

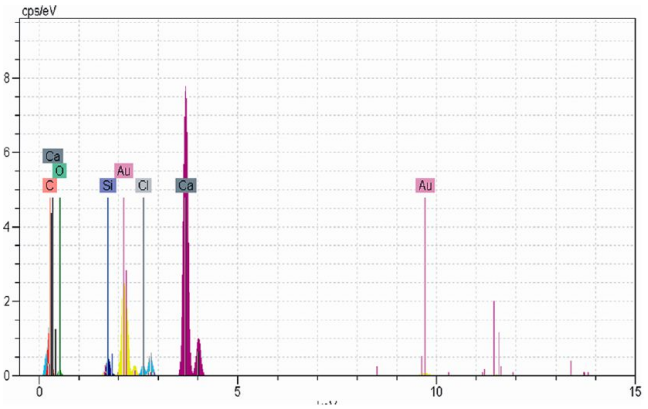

a) prior to oil flooding

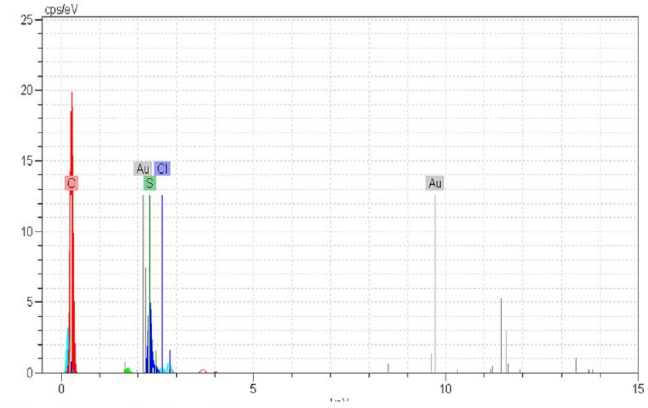

b) after oil flooding

Figure 7. Elemental analysis of carbonate core sample.

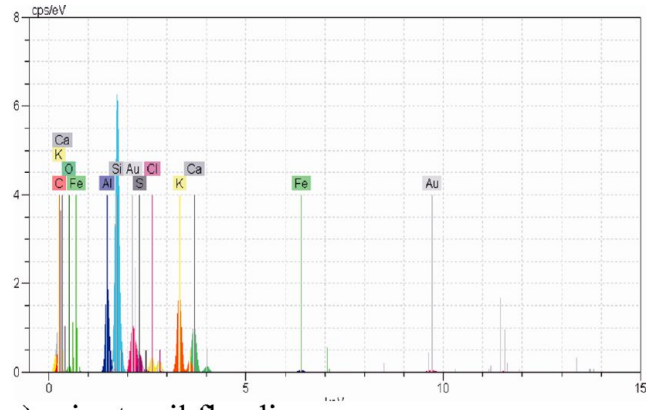

a) prior to oil flooding

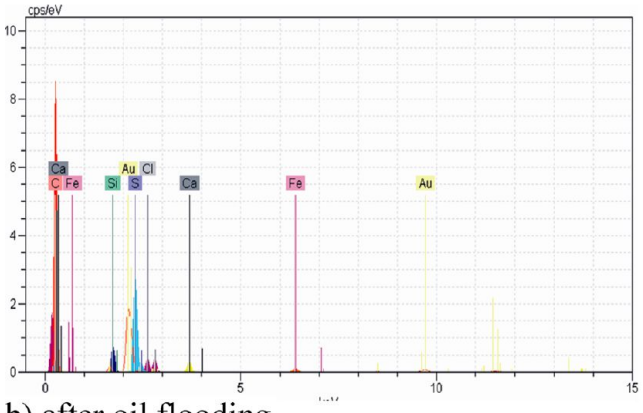

b) after oil flooding

Figure 8. Elemental analysis of sandstone core sample.

Water phase

$$\frac{\partial}{\partial t}(\phi S_{\mathrm{W}}\rho_{\mathrm{W}}w_{\mathrm{WL}}) + \frac{\partial}{\partial x}(\rho_{\mathrm{W}}u_{W}w_{WL}) = 0 \tag{11}$$

The saturations of phases are given:

$$S_{\mathrm{L}} + S_{\mathrm{V}} + S_{\mathrm{W}} = 1 \tag{12}$$

The momentum balance equation is given by Darcy's law

$$u_{\mathrm{L}} = -\frac{k}{\mu_{\mathrm{L}}}\frac{\partial P}{\partial x} \tag{13}$$

Therefore, in this work the instantaneous local porosity during asphaltene deposition is proposed to be difference between the initial porosity ($\varnothing_0$) and the fractional pore volume occupied by the deposited asphaltene (E_{A}) and also adsorbed asphaltene as multilayer (E_{AA}) in the developed model:

$$\varnothing = \varnothing_0 - E_{\mathrm{A}} - E_{\mathrm{AA}} \tag{14}$$

The instantaneous, local permeability, k, is calculated by[28]

$$k = k_0\left(\frac{\varnothing}{\varnothing_0}\right)^m \tag{15}$$

The boundary and initial conditions can be considered as

$$C_{\mathrm{A}} = 0 \qquad 0 \le x \le L \qquad t = 0 \tag{16}$$

$$E_{\mathrm{A}} = 0 \qquad 0 \le x \le L \qquad t = 0 \tag{17}$$

$$\text{Ø} = \varnothing_0 \qquad 0 \le x \le L \qquad t = 0 \tag{18}$$

$$k = k_0 \qquad 0 \le x \le L \qquad t = 0 \tag{19}$$

3.5. Thermodynamic Modeling. According to Flory–Huggins theory,[29,30] the chemical potential of the asphaltene component is calculated as follows:

$$\frac{(\mu_{\mathrm{p}} - \mu_{\mathrm{p}}^{0})}{RT} = \ln \Phi_{\mathrm{p}} + \left(1 - \frac{v_{\mathrm{p}}}{v_{\mathrm{s}}}\right)\Phi_{\mathrm{s}} + \frac{v_{\mathrm{p}}}{RT}[(\delta_{\mathrm{p}} - \delta_{\mathrm{s}})\Phi_{\mathrm{s}}]^2 \tag{20}$$

The solubility parameter in eq 1 is written as below:

$$\delta_i = \left(\frac{\Delta u}{v}\right)^{0.5} \tag{21}$$

The values of Δu and v are calculated by the Soave–Redlich–Kwong equation of state (SRK EOS). In this work, it is assumed that the asphaltene phase is as a pseudocomponent liquid in which asphaltene precipitation has no effect on liquid–vapor equilibrium. Also, crude oil is considered as a binary homogeneous mixture of asphaltene and solvent. By equating the fugacity of asphaltene in liquid and solid phase, we have:

$$\Phi_{\mathrm{p}}^{\mathrm{L}} = \exp\left(\frac{v_{\mathrm{p}}^{\mathrm{L}}}{v^{\mathrm{L}}} - 1\right)\Phi_{\mathrm{s}} - \frac{v_{\mathrm{p}}^{\mathrm{L}}}{RT}(\delta_{\mathrm{p}} - \delta_{\mathrm{s}})^2\Phi_{\mathrm{s}}^2 \tag{22}$$

The weight fraction of asphaltene precipitation is calculated as below:

$$W_{\mathrm{SAL}} = \frac{(1 - \Phi_{\mathrm{p}}^{\mathrm{L}})(M_{\mathrm{W}}^{\mathrm{L}}/v^{\mathrm{L}})}{(1 - \Phi_{\mathrm{p}}^{\mathrm{L}})(M_{\mathrm{W}}^{\mathrm{L}}/v^{\mathrm{L}}) + (\Phi_{\mathrm{p}}^{\mathrm{L}})(M_{\mathrm{Wp}}/v_{\mathrm{p}})} \tag{23}$$

dx.doi.org/10.1021/ef3017255 | *Energy Fuels* 2013, 27, 622–639

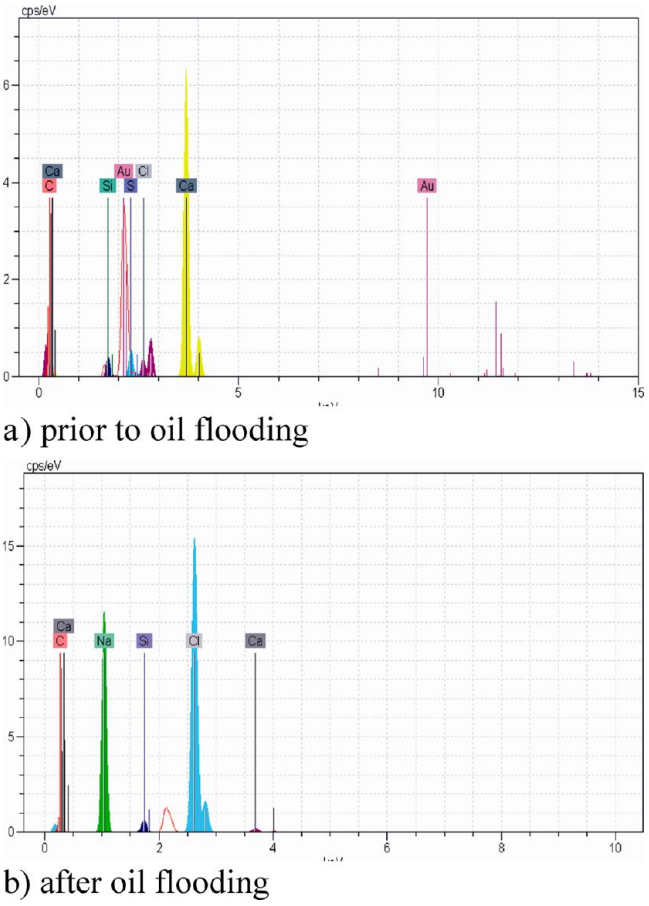

Figure 9. Elemental analysis of dolomite core sample.

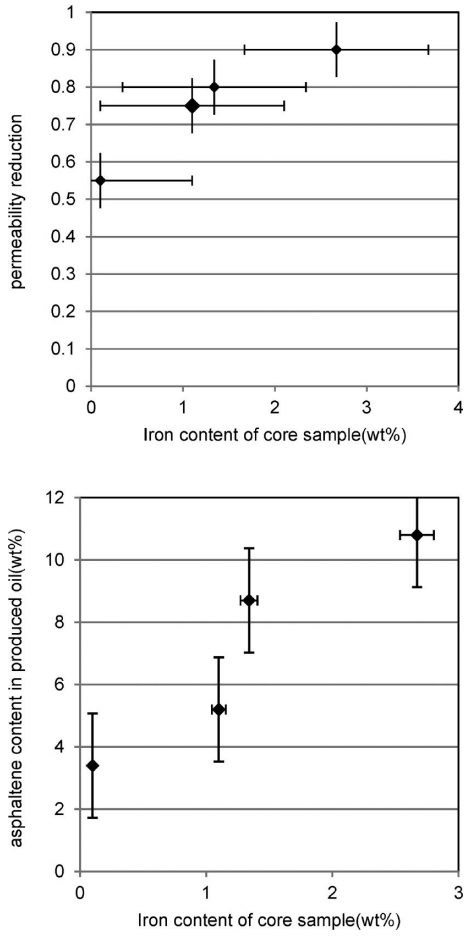

Figure 10. Effect of iron content of core sample on the permeability damage and asphaltene content of produced oil.

3.6. Model Validation. To validate the proposed model for calculating permeability damage due to asphaltene deposition in different porous media, numerical simulation runs were conducted for nine oil flooding experiments performed in this work and six oil flooding experiments given in the literature.[8] The description of the performed experiments are given in Tables 7 and 8. Experimental permeability damages due to asphaltene deposition in the core were correlated using the developed model of asphaltene deposition, and their coefficients were adjusted to achieve best match with the experimental data. The partial differential eqs 2, 4, 6, and 9−11 were coupled and discretized using the Crank−Nicholson method, central difference in space, and trapezoidal rule in time, giving second-order convergence in time, and solved in MATLAB software to determine pressure and asphaltene concentration along the core samples. The Rung−Kutta fourth-order scheme has been applied to calculate the volume fraction of asphaltene deposition and adsorption. A fully implicit numerical model was performed and solved by iteration. Numerical simulation runs were conducted to obtain the best match between experimental and numerical results. Numerical simulation was carried out in a linear grid system of 80 grid blocks. Time was discretized with a Δt of 40 s. For optimization and determination of the model parameters, history matching was used. In this study, the square root of the summation of differences between measured and calculated porosity data were defined as the objective function:

$$\text{objective function} = \sqrt{\sum_{i=1}^{n}\left(\left(\frac{k}{k_0}\right)_{\text{meas}} - \left(\frac{k}{k_0}\right)_{\text{calc}}\right)^2} \quad (24)$$

As a result, the model parameters obtained by optimization procedure are Γ_∞, n, m, α, β, k_1, k_2, v_c, γ, and σ.

4. RESULTS AND DISCUSSION

4.1. Effect of Asphaltene Deposition on Morphology of Core Sample. The core samples were damaged in the natural depletion process mentioned previously, and a deposited carbon layer was formed on the surface after flooding. The morphology and particle size of deposited carbon formed on carbonate, sandstone, and dolomite core samples by scanning electron microscopy (SEM) are given in Figures 4−6 before and after flooding. The SEM image gives a three-dimensional view of the core sample at a microscopic level. The reduction in permeability is caused due to deposited carbon blocking the pore throats as shown in the SEM images. The amount of carbon deposition can vary in within the sandstone and carbonate core samples. Carbonate and dolomite core samples taken after the oil flooding experiments present less black area (evidence of the porosity reduction), while no discernible holes are present, but represent that the surfaces seem rougher due to the deposited carbon in comparison to sandstone core samples. These results show that deposited carbon tends to more adsorb throughout the carbonate and dolomite core samples more than the sandstone core sample due to the existence of more active sites for carbon adsorption. SEM images show that the dispersed groups of deposited carbon aggregate together and forms layers on the surface of the rock sample that cover the

dx.doi.org/10.1021/ef3017255 | Energy Fuels 2013, 27, 622−639

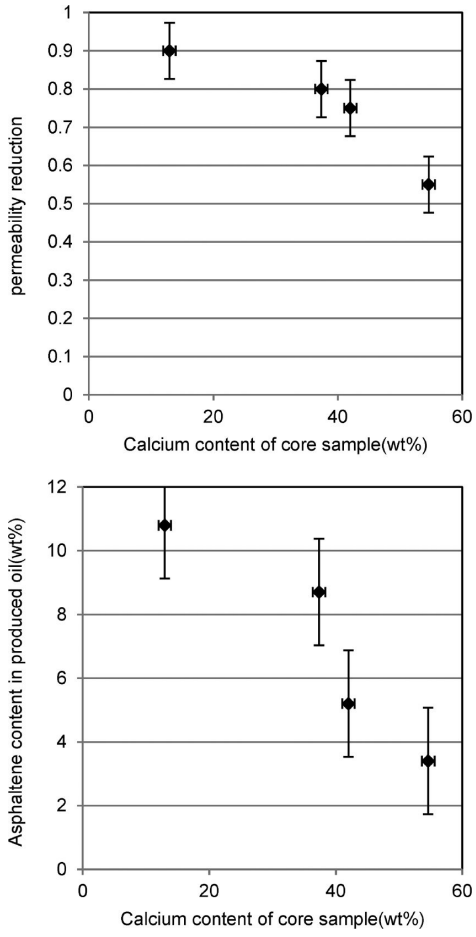

Figure 11. Effect of calcium content in the core sample on the permeability damage and asphaltene content of produced oil.

surface of the rock sample. Thus, the carbonate core samples experienced more particle plugging compared to sandstone core samples and the carbonate core samples severely plugged by carbon deposition. It can be also found that the carbon deposition has different mechanisms in carbonate and sandstone core samples and hydrocarbon deposition in carbonate core sample is more important than that in sandstone core sample. Also, SEM analyses of carbon deposition on surface carbonate core samples show the formation of large clusters on the layers of deposited carbon already adsorbed on the surface of carbonate rock with characteristic sizes that greatly exceed the monolayer characteristic size. Therefore, these experimental results suggest multilayer deposition of carbon on carbonate core samples. The EDX analyses show more carbon deposition in studied carbonate core sample in comparison to that in studied sandstone core sample was observed. Considering the reservoir temperature, this carbon element can be assumed to be produced from deposited asphaltene.[31]

4.2. Effect of Mineral Composition on Asphaltene Deposition. The deposition and adsorption of asphaltene depend on the core structure, mineral composition, and consolidation of core samples. In the majority existing work, the effect of mineral composition on asphaltene deposition was not investigated. In this work, the effect of mineral composition on asphaltene deposition was studied using elemental analyses of core samples and X-ray fluorescence (XRF) analysis. Table 4 indicates the results of XRF analysis for studied core samples. These results show that the iron content of studied cores is

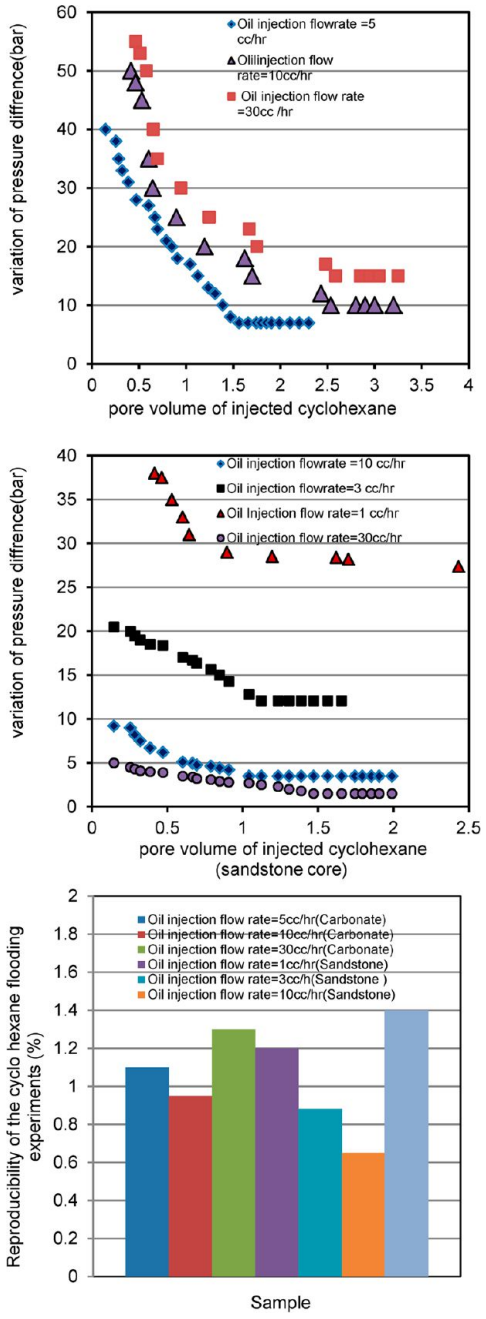

Figure 12. Variation of pressure drop through damage removal due to mechanical plugging and reproducibility of the experiments.

from 0.1 to 3.65 wt %. The iron content of sandstone core samples is 2.67 and 3.65 wt %, whereas the iron content of the carbonate core sample is negligible. Also, the calcium contents of carbonate and dolomite core samples are 54.6% and 37.35% respectively, which are more than those of sandstone core samples. The results obtained from XRF analysis show more iron content and less calcium content in sandstone core samples in comparison to carbonate core sample. Figures 7−9 show the elemental analyses of core samples prior and after crude oil flooding. A significant increase in the amount of carbon was counted after oil flooding, which again confirms the deposition of asphaltene in the pores of the core samples. The EDX analyses show the more asphaltene deposition in studied carbonate core sample in comparison to studied sandstone core sample.

dx.doi.org/10.1021/ef3017255 | *Energy Fuels* 2013, 27, 622−639

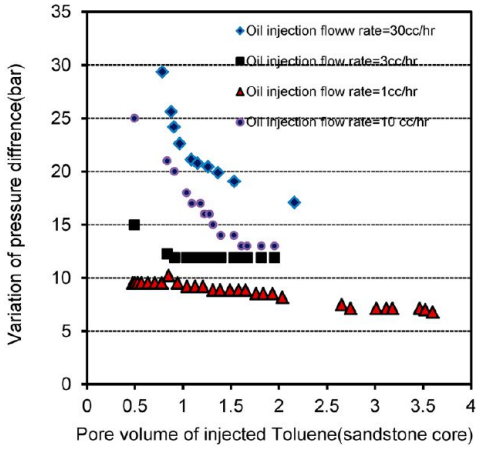

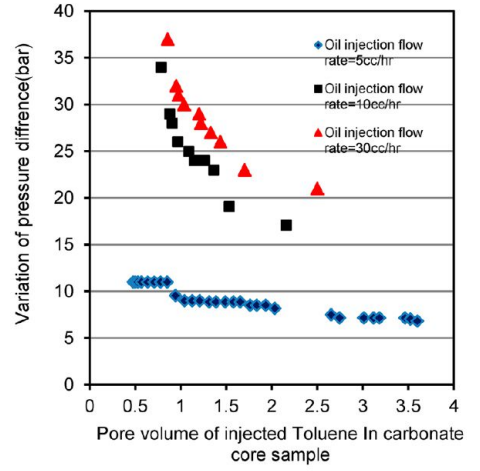

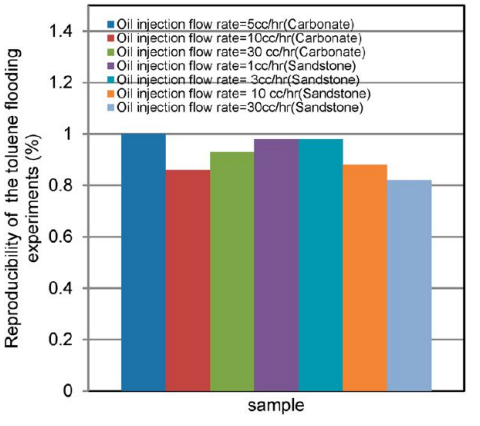

Figure 13. Variation of pressure drop through damage removal due to adsorption mechanism and reproducibility of the experiments.

Another important observation is that an increase of the iron content of core leads to a less permeability damage and an increase in the core calcium content leads to an increase of the permeability damage during natural depletion due to asphaltene deposition as shown in Figures 10 and 11 and Table 4. Asphaltene is a positive polar component; therefore, carbonate formations have higher ability than sandstone formation to adsorb asphaltene due to more calcium content. In fact, the existence of polar components make the asphaltene molecules tend to strongly adhere to the surface and, hence, lead increase in to the amount of asphaltene deposition on the surface of the carbonate rock samples. As a matter of fact, the carbonate core inner surface may contain polar groups as

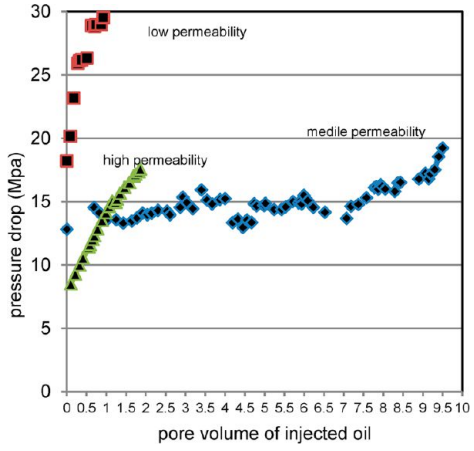

Figure 14. Variation of pressure drop versus injected pore volume for studied cores.

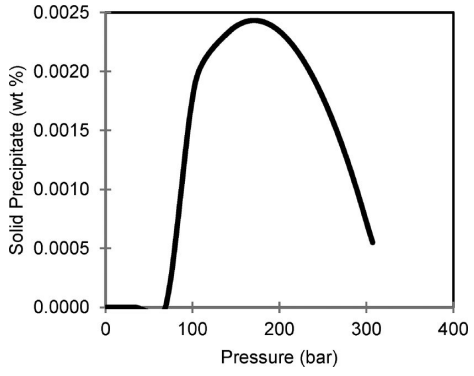

Figure 15. Asphaltene precipitation modeling of studied bottom hole live oil.

calcite, which can exert polar interactions with asphaltenes surface groups.

4.3. Deposited Asphaltene Measurement Due to Mechanical Plugging Mechanism Using Cyclohexane Flooding. The results of formation damage due to asphaltene deposition by the mechanism of mechanical trapping and recovery of damage are shown in Tables 7 and 8 and Figure 12. Table 7 indicates that 60−82% of the total damage is due to mechanical plugging and can be recovered by simple reverse flow of cyclohexane. Therefore, the mechanical plugging is the dominant mechanism of permeability damage during natural depletion. Due to neutrality of cyclohexane on asphaltene precipitation/dissolving, cyclohexane reversal flooding removes the deposited asphaltene on the surface due to mechanical trapping mechanism. Hence, the measured concentration of asphaltene in cyclohexane solution (measured by spectrophotometer), after reaching a stable differential pressure in cyclohexane reverse flooding, introduces the amount of deposited asphaltene by mechanical plugging mechanism as shown in Table 7. Also, Table 7 indicates that an increase in oil injection flow rate is followed by an increase in amount of deposited asphaltene due to mechanical plugging mechanism which is more than those obtained by the adsorption mechanism. Figure 12 shows the variation of pressure due to reversal flow of cyclohexane in sandstone and carbonate core samples, respectively. It can be found that deposited asphaltene by mechanical plugging mechanism can be removed by cyclohexane reverse flooding. The removal of damage by a mechanical

dx.doi.org/10.1021/ef3017255 | Energy Fuels 2013, 27, 622−639

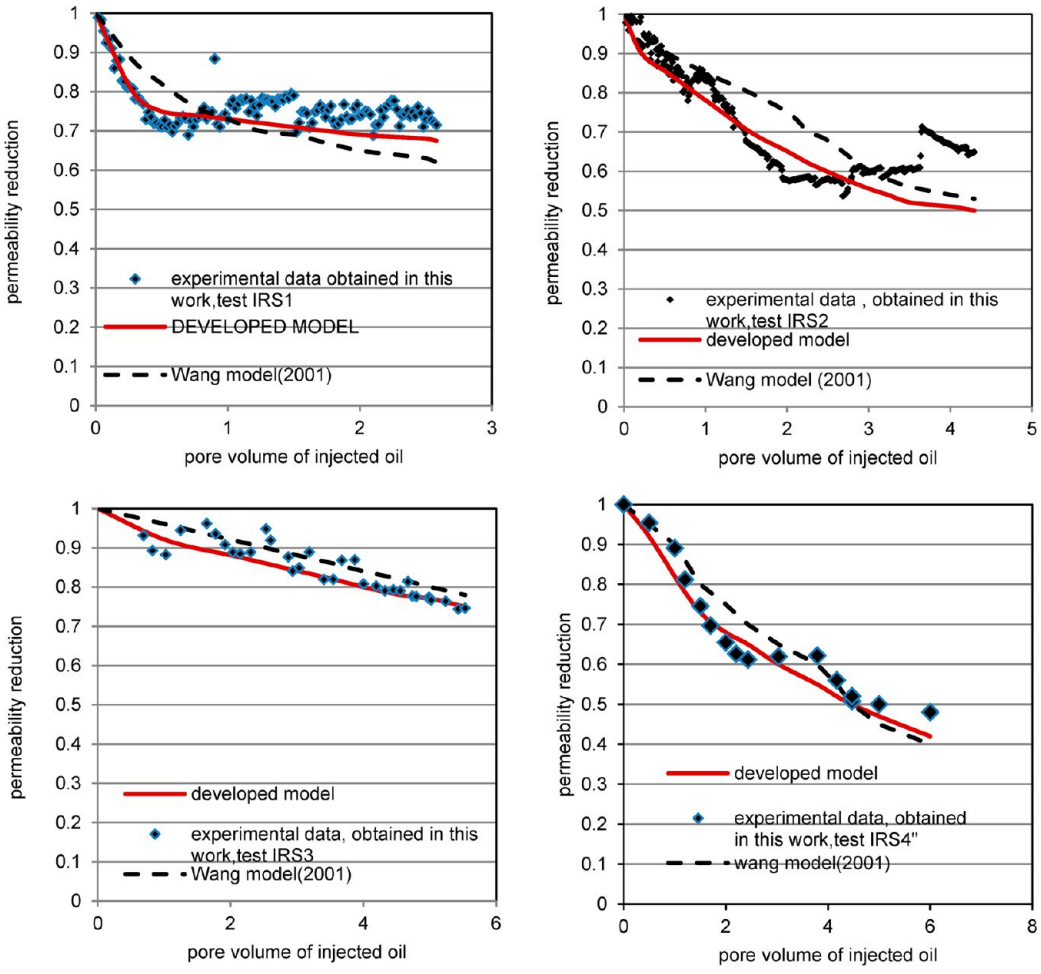

Figure 16. Aphaltene deposition modeling for studied sandstone core samples.

plugging mechanism using the reverse cyclohexane flooding takes in a very short time about two pore volume injections. Asphaltene is a positive polar component; therefore, carbonate formations have higher ability than sandstone formation to adsorb asphaltene. In fact, the existence of polar components make the asphaltene molecules tend to strongly adhere to the surface and, hence, lead increase in to the amount of asphaltene deposition on the surface of the carbonate rock samples. As a matter of fact, the carbonate core inner surface may contain polar groups, which can exert polar interactions with asphaltene surface groups. Hence, the initial pressure drop increases for flow rates increasing in the carbonate core sample. While the surface of the sandstone rock samples has no polar groups, therefore, the pressure drop increases with applied flow rates decrease.

The numerical results characterizing the reproducibility of the cyclohexane flooding experiments are summarized in Table 8 and Figure 12. The results show that the reproducibility of the cyclohexane experiments is around 0.65−1.4% for sandstone core sample and 0.95−1.3% for carbonate core sample.

4.4. Deposited Asphaltene Measurement Due to Adsorption Mechanism Using Toluene Flooding. The results of formation damage due to asphaltene deposition by the mechanism of adsorption and removal of damage are shown in Tables 7 and 8 and Figure 13. As shown in Table 6, the contribution of this mechanism is about 18−40% of the total percentage of permeability reduction. It can be found that deposited asphaltene because of the adsorption mechanism can be removed by toluene reverse flooding. Due to reaction of toluene with adsorbed asphaltene on active sites of the core sample, toluene reverse flooding removes the adsorbed asphaltene by an adsorption mechanism from active sites of core samples. Thus, the concentration of asphaltene in toluene solution (measured by spectrophotometer) introduces the amount of deposited asphaltene by an adsorption mechanism. In fact, the removal of damage by the asphaltene adsorption mechanism by toluene reverse flooding occurs over a long time, about 3.7 pore volume injections. Also, Table 7 shows a decrease in the adsorbed amount of asphaltene with an increase in flow rate of oil injection. It can be concluded that formation damage due to asphaltene adsorption in carbonate core sample under dynamic condition is more than in sandstone core sample which is due to more active sites for adsorption of asphaltene in carbonate core samples. These observations which are related to the interactions between the asphaltene functional groups and the core surface involve surface polarity, affinity, or other attractive forces. As explaned in a previous section, these interactions are related to the core structure, mineral composition, and consolidation of core samples. Permeability reduction by asphaltene deposition was caused by the mechanical plugging mechanism during a fast process, while formation damage due to the adsorption mechanism takes place in a longer time. Hence, the pressure drop increases with increasing flow rate in each core sample. The numerical

dx.doi.org/10.1021/ef3017255 | *Energy Fuels* 2013, 27, 622−639

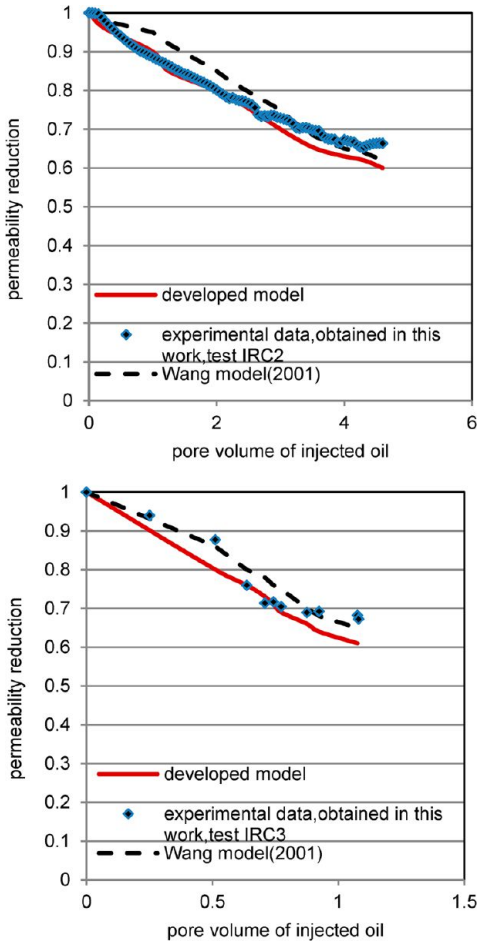

Figure 17. Aphaltene deposition modeling for studied carbonate core samples.

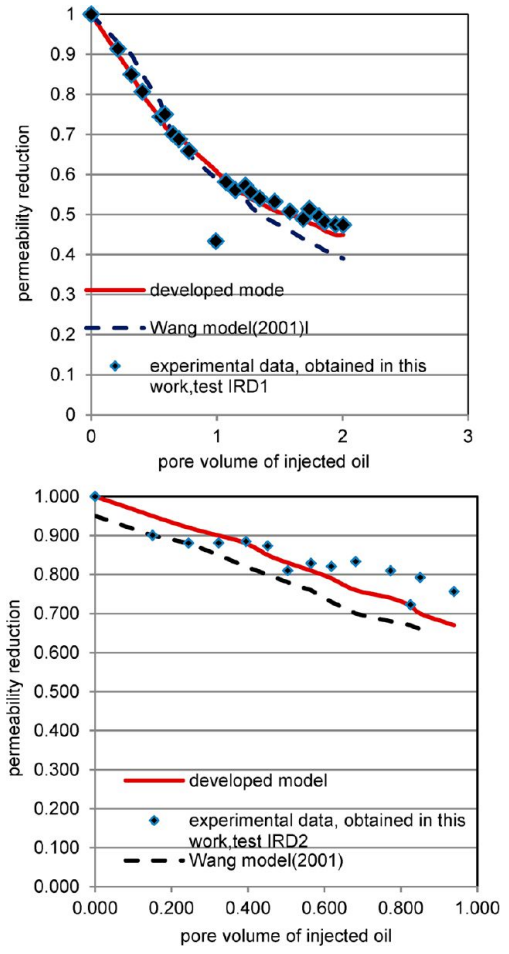

Figure 18. Aphaltene deposition modeling for studied dolomite core samples.

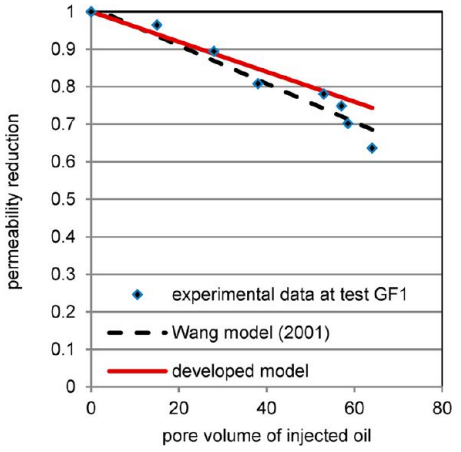

Figure 19. Aphaltene deposition modeling for sample GF1.

results characterizing the reproducibility of the toluene flooding experiments are summarized in Table 8 and Figure 13. The results show that the reproducibility of the toluene experiments is around 0.82−0.98% for the sandstone core sample and 0.86−1.0% for the carbonate core sample.

In our previous work, the pressure drop resulting from oil flow inside the core sample due to asphaltene deposition was shown completely.[32] However, in order to compare, Figure 14 shows the pressure drop versus pore volume for three rocks with different permeability. It can be concluded that the formation damage caused by asphaltene deposition in the low permeability rock was more severe than that in higher permeability rock for the same asphaltene content of the crude oil and under the same dynamic potential force. For the low permeability core sample, there may be a continuous deposition until complete plugging. In the low permeability core, the plugging mechanism acts like a snowball growth that can be inferred from the sharp slopes of the Figure 14 once plugging deposition is activated leading to the first significant pressure variation. In the high permeability core, the region of the asphaltene deposition was limited in the inlet end of the core. Finally, there can be a steady deposition until interstitial velocity is high enough not to allow further mechanical plugging for medium permeability core.

4.5. Developing Model. It is important to note that the permeability reduction was not only a result of fines migration in the rock but also a result of the asphaltene adsorption mechanism. In the majority of previous models, the asphaltene deposition is based on the Gruesbeck and Collins experiments[7] for fine mineral particle migration and also only two material balance equations were applied. Therefore, the previous models in the literature are based on the mechanical trapping mechanism and do not consider the adsorption mechanism which is related to interactions between the positive polar component of asphaltenes and the rock surface.

According to the SEM analysis of the asphaltene adsorption on core samples, it can be observed that asphaltene deposition

dx.doi.org/10.1021/ef3017255 | Energy Fuels 2013, 27, 622−639

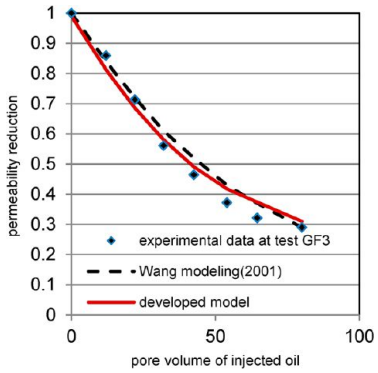

Figure 20. Aphaltene deposition modeling for sample GF3.

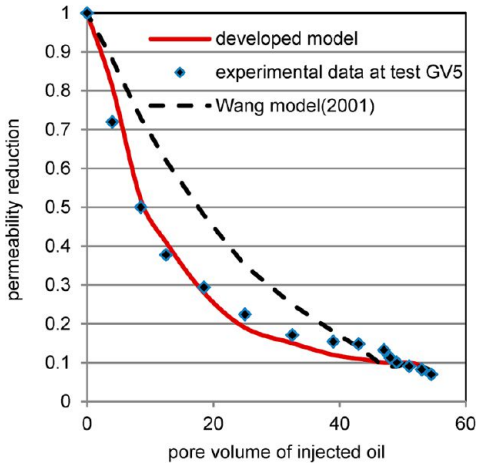

Figure 21. Aphaltene deposition modeling for sample GV5.

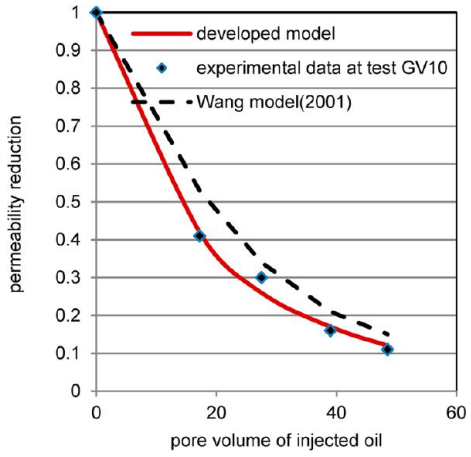

Figure 22. Aphaltene deposition modeling for sample GV10.

with characteristic sizes that greatly exceeds the monolayer size in particular on carbonate core sample was formed. Therefore, in the proposed asphaltene deposition model in this work, in addition to mechanical plugging mechanism term according to the Wang model,[15] a multilayer adsorption kinetic mechanism term for asphaltene was included. Also, application of four material balance equations (oil, asphaltene, gas components, and water phase) instead of two material balance equations was considered. The main objective of this section is to compare the performance and the capabilities of the proposed model based on the multilayer adsorption kinetic mechanism and the Wang

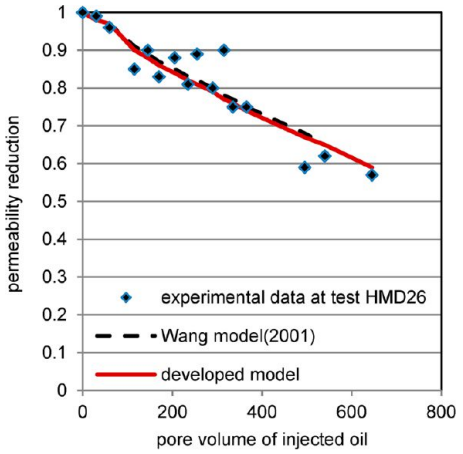

Figure 23. Aphaltene deposition modeling for sample HMD26.

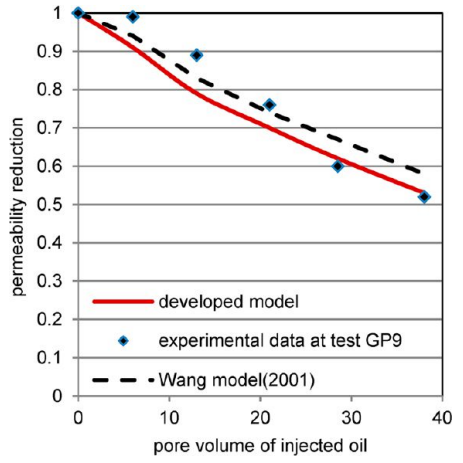

Figure 24. Aphaltene deposition modeling for sample GP9.

model based on the mechanical plugging mechanism in more detail. In this work, for thermodynamic modeling of asphaltene precipitation at different pressures, the Flory–Huggins theory[29] was used as shown in Figure 15.

The proposed model was correlated using the oil flooding experimental data obtained in this work which are denoted as IRS1–IRD2. Figures 16–18 compare the results of permeability reduction in the sandstone, carbonate, and dolomite core samples due to the asphaltene deposition using the proposed model with those obtained from the Wang model. It should be noted that the performance of the proposed model was also checked and compared with that of the Wang model using the experimental data given by Minssieux et al.[8] as shown in Figures 19–24.

Figures 19–24 show that the proposed model can correlate more accurately the experimental data in comparison to the Wang model.

Table 9 shows the average absolute deviation (AADs) of the predicted permeability reduction from the experimental data due to asphaltene deposition using the proposed model and that of the Wang model. These results confirm also that the proposed model based on the multilayer adsorption mechanism of asphaltene is capable of correlating the permeability reduction experimental data with AADs of 1.2–1.9%, whereas the Wang model correlates less accurate asphaltene deposition with AADs of 4.2–5.4%. Also, the obtained results indicate that the

dx.doi.org/10.1021/ef3017255 | Energy Fuels 2013, 27, 622–639

Table 9. Absolute Deviation of the Correlated Permeability Reduction from the Experimental Results by the Proposed Model and the Wang Model

	Absolute Average Deviation of Asphaltene Deposition Modeling (%)								
	sandstone core sample (3)			carbonate core sample			dolomite core sample		
oil injection flow rate (cm^3/h)	developed model	Wang model	model in SPE paper[35]	developed model	Wang model	model in SPE paper[35]	developed model	wang model	model in SPE paper[35]
1	2.1	4.2	3.9						
3	2.4	4.4	4.6				1.5	5.1	4.4
5				1.2	5.4	4.9	1.6	4.8	4.3
10	2.3	4.5	4.7	1.4	4.8	5.1			
30	2.5	4.8	4.5						

Table 10. Adjusted Parameters of the Proposed Model

	Oil Injection Rate (cm^3/h)							
	sandstone core sample				carbonate core sample		dolomite core sample	
adjusted parameter	1	3	10	30	5	10	3	5
α	0.034	0.046	0.062	0.084	0.089	0.093	0.042	0.074
β	0.04	0.046	0.051	0.074	0.52	0.62	0.092	0.098
v_c	0.042	0.036	0.023	0.019	0.028	0.015	0.016	0.012
γ	0.041	0.048	0.055	0.068	0.39	0.46	0.063	0.084
Γ_∞	164.2	164.2	164.2	164.2	132.4	132.4	138.8	138.8
k_1	0.0025	0.0028	0.0036	0.0041	0.074	0.097	0.076	0.084
k_2	2.6×10^{-4}	4.8×10^{-4}	6.4×10^{-4}	8.1×10^{-4}	6.4×10^{-3}	7.4×10^{-3}	5.8×10^{-3}	7.1×10^{-3}
n	11	12	14	16	7	8	6	7
m	34	35	38	41	44	46	39	41

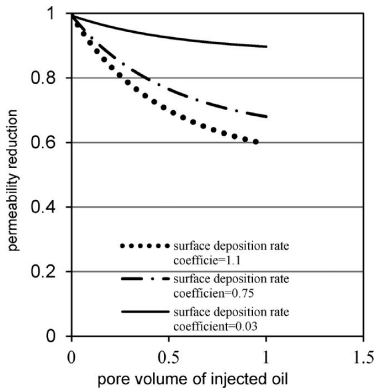

Figure 25. Effect of surface deposition rate coefficient on permeability reduction.

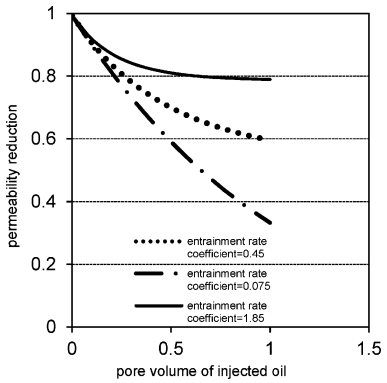

Figure 26. The effect of entrainment rate coefficient on permeability reduction.

proposed model can correlate better the asphaltene deposition experimental data on carbonate and dolomite core samples during flooding with AADs of 1.2−1.4% in comparison to sandstone core samples with AADs of 1.5−1.9%. This suggests that the multilayer adsorption mechanism of asphaltene has an important role in asphaltene deposition in carbonate and dolomite samples. Also, according to our previous publication,[33,34] the multilayer adsorption mechanism of asphaltene is important in CO_2 flooding and natural depletion phenomenon. This phenomenon can be justified by the fact that the asphaltene adsorption mechanism, which is related to the interactions between the asphaltenes functional groups and the core surface, involves surface polarity, affinity, or other attractive forces. It is also known that asphaltene surface groups may have acidic (carboxylic, benzoic, phenolic) and/or basic (pyridine, pyrazine, dimethylsulfoxide) functionality.[35] Also, Table 9 shows the average absolute deviations (AADs) of the predicted permeability reduction from the experimental data due to asphaltene deposition using a model presented in a SPE paper.[36]

Table 10 shows the adjusted parameter values of the proposed model based on the multilayer adsorption kinetic mechanism of asphaltene during dynamic conditions in porous media. It should be noted that the adjusted parameters are affected by the process parameters (temperature, particle size, flow regime, etc) and also the nature of the porous medium (rock morphology, rock-surface characteristics, mineral composition, etc). For example, the adjusted parameters in the proposed model as the first adsorption step parameter (k_1) and the second adsorption step parameter (k_2) have different quantities in carbonate and sandstone core samples which is related to different mineral composition and rock morphology.

4.6. Sensitivity Analysis. The asphaltene deposition model includes some parameters that control the deposition of asphaltene. Sensitivity analysis was performed to investigate the effect of each parameter on asphaltene deposition in natural

dx.doi.org/10.1021/ef3017255 | Energy Fuels 2013, 27, 622−639

depletion processes. These parameters are the surface deposition rate coefficient (α), the entrainment rate coefficient (β), the pore throat plugging rate coefficient (γ), and the critical interstitial velocity (v_c).

Figure 25 shows the effect of surface deposition rate coefficient on permeability reduction. It can be concluded that permeability reduction increases as the value of surface deposition rate coefficient increases. Therefore, plugging of the formation is expected during asphaltene adsorption on the reservoir rock.

Figure 26 indicates the effect of entrainment rate coefficient on permeability reduction. It can be seen that the permeability reduction decreases with increasing entrainment rate coefficient. The entrainment and surface deposition mechanisms proceed against each other. So, in most situations one of these two mechanisms is dominant, and the other one might be ignored. It should be noted that the entrainment mechanism is activated at high flow rates.

The effects of pore throat plugging coefficient on asphaltene deposition was shown in Figure 27. The results indicate that

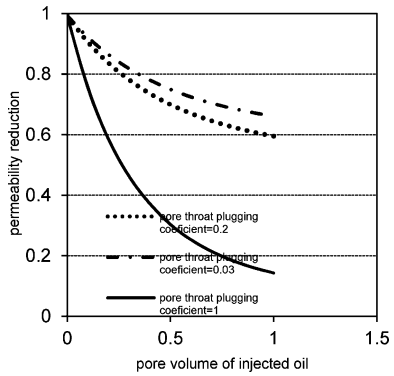

Figure 27. Effects of pore throat plugging coefficient on permeability reduction.

when the pore throat plugging coefficient increases deposition of asphaltene at the pore throat increases. Due to this mechanism, partial or total pore plugging is expected.

Figure 28 represents the effect of critical velocity on permeability reduction When v_c increases, deposited asphaltene

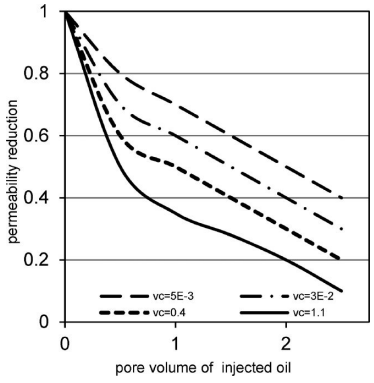

Figure 28. Effect of critical velocity on permeability reduction.

increases. Asphaltene deposition continues when the interstitial velocity is less than v_c. At critical velocity, the entrainment mechanism is dominant, so the deposited asphaltene decreases.

5. CONCLUSIONS

A new asphaltene deposition model based on a multilayer adsorption kinetic mechanism and four material balance equations (oil, asphaltene, gas, and water phase) was developed to account for permeability reduction in porous media during dynamic conditions, and the model was verified using experimental data obtained in this work and also found in the literature. A sensitivity analysis was also done to investigate the effect of each parameter on the asphaltene deposition.

In this work, a set of experiments was conducted using a bottom hole live oil sample under dynamic conditions in porous media with the purpose of distinguishing between mechanical plugging and adsorption mechanisms involved in the interfacial interaction of the asphaltene/mineral rock system using a proposed procedure based on cyclohexane or toluene reverse flooding. The effective parameters of porous media on asphaltene deposition as mineral composition and morphology of the surface were studied in this work using X-ray, elemental analysis, and SEMs. The experimental and modeling results of asphaltene deposition and adsorption during core flooding lead to the following conclusions.

1. The proposed model based on a multilayer adsorption kinetic mechanism of asphaltene and four material balance equations given in this work is found to be more accurate than the Wang model based on the mechanical plugging mechanism with AADs less than 1.9%, especially in carbonate and dolomite core samples. Hence, the multilayer adsorption kinetic mechanism of asphaltene plays an important role in asphaltene deposition, permeability reduction, and wettability alteration of reservoir rock.
2. The experimental results show that an increase in oil injection flow rate is followed by an increase in pressure drop and permeability reduction of core sample.
3. SEMs of asphaltene deposition on surface carbonate core samples show the formation of large clusters with characteristic sizes that greatly exceed the monolayer characteristic size and propose multilayer adsorption of asphaltene on porous media.
4. It was also found that an increase in iron content of the core leads to less permeability damage and an increase in calcium content of the core leads to an increase in permeability damage during natural depletion due to asphaltene deposition.
5. The experimental data indicate that 60−80% of the total damage is due to mechanical plugging and can be recovered by cyclohexane reverse flooding rapidly.
6. The experimental results show that the contribution of adsorption mechanism in permeability reduction is about 20−40% of the total percent permeability reduction and deposited asphaltene by adsorption mechanism can be removed slowly by toluene reverse flooding.
7. It can be concluded from sensitivity analysis that permeability reduction increases as the value of the surface deposition rate coefficient and pore throat plugging coefficient increase. Also, the permeability reduction decreases with increasing entrainment rate coefficient.

AUTHOR INFORMATION

Corresponding Author

*Tel.: +98 21 66165424. Fax: +98 21 66022853. E-mail: Ghotbi@sharif.edu.

Notes

The authors declare no competing financial interest.

■ ACKNOWLEDGMENTS

The sponsorship of this research by the Research Institute of the Petroleum Industry (RIPI) is gratefully acknowledged.

■ NOMENCLATURE

C = the volume fraction of the suspended asphaltene precipitates in the liquid phase
D_{pt} = the average pore throat diameter
D_{ptcr} = the critical pore throat diameter, assumed constant
E_A = volume of asphaltene deposited per unit initial volume, dimensionless
E_{AA} = volume of asphaltene adsorbed per unit initial volume, dimensionless
f = fugacity
k = permeability
k_1 = the first adsorption step parameter (this step is taken to be adsorption of asphaltenes in solution to the surface of the rock)
k_2 = the second adsorption step parameter (this step is taken to be the adsorption of asphaltenes in solution to those asphaltenes already adsorbed to the rock)
R = gas constant
m = power-law exponent, dimensionless
n = the mean aggregation number of the adsorbed asphaltenes (in developed model)
u = internal energy
u_L = the flux of the liquid phase
v = molar volume
v_L = the interstitial velocity of liquid phase
v_c = the critical interstitial velocity of liquid phase, cm/s
w_{AL} = the dissolved asphaltene in the liquid phase
wasp = asphaltene content of the bottom hole live oil
w_G = the mass fraction of gas
w_{OL} = the mass fraction of the oil in the liquid phase
w_{SAL} = the mass fractions of the suspended asphaltene precipitates
w_{WL} = the mass fraction of water in liquid phase

Greek Symbols

$\varnothing$ = porosity
μ = viscosity
ρ = density
Γ = mg of asphaltene/m^2
Γ_∞ = the maximum possible adsorption for the whole isotherm
α = surface deposition rate coefficient, 1/s
β = entrainment rate coefficient, 1/cm
γ = plugging deposition rate coefficient, 1/cm
σ = the snowball-effect deposition constant
μ_p = chemical potential

Subscripts

cal = calculated
exp = exponential function
O = the oil phase
pres = reservoir pressure
Q = flow rate
T_{res} = reservoir temperature

■ REFERENCES

(1) Mullins, O. C.; Sheu, E. Y.; Hammami, A.; Marshal, A. G. *Asphaltenes, Heavy Oils and Petroleomics*; Springer: New York, 2007; pp 259.
(2) Sarma, H. K. Can We Ignore Asphaltene in a Gas Injection Project for Light-Oils? *SPE International Improved Oil Recovery Conference*, Kuala Lumpur, Malaysia, October 20−21, 2003; SPE 84877.
(3) Bagheri, M. B.; Kharrat, R.; Ghotbi, C. *Rev. Inst. Fr. Pet.* **2011**, *66* (3), 1−13.
(4) Sim, S. S. K.; Takabayashi, K.; Okatsu, K.; Fisher, D. Asphaltene-Induced Formation Damage: effect of Asphaltene Particle size and core permeability. *SPE Annual Technical Conference*, Dallas, Texas, USA, October 9−12, 2005; SPE 95515.
(5) Hamadou, R.; Khodja, M.; Kartout, M.; Jada, A. *Fuel* **2008**, *87*, 2178−2185.
(6) Ali, M. A.; Islam, M. R. The effect of asphaltene precipitation on carbonate rock permeability: An experimental and numerical approach. *SPE Annual Technical Conference and Exhibition*, San Antonio, October 5−6, 1997; SPE 38856.
(7) Gruesbeck, C.; Collins, R. E. *Soc. Pet. Eng. J.* **1982**, *22*, 847−856.
(8) Minssieux, L.; Nabzar, L.; Chauveteau, G.; Longeron, D.; Bensalem, R. *Rev. Inst. Fr. Pet.* **1998**, *53* (3), 313−327.
(9) Leontaritis, K. J. Asphaltene near-wellbore formation damage modeling. *Formation Damage Control Conference*, Lafayette, LA, February 18−19, 1998; SPE 39446.
(10) Civan, F. Modeling and simulation of formation damage by organic deposition. *First International Symposium on Colloid Chemistry in Oil Production: Asphaltene and Wax Deposition*, Rio de Janeiro, Brazil, November 26−29, 1995.
(11) Wang, S.; Civan, F.; Strycker, A. R. Simulation of paraffin and asphaltene deposition in porous media. *SPE International Symposium on Oilfield Chemistry*, Houston, TX, February 16−19, 1999; SPE 50746.
(12) Nghiem, L.; Kohse, B. F.; Ali, S. M. F.; Doan, Q. Asphaltene precipitation: phase behavior modeling and compositional simulation. *Asia Pacific Conference on Integrated Modeling for Asset Management*, Yokohama, Japan, April 25−26, 2000; SPE 59432.
(13) Kumar, T.; Todd, A. C. A new approach for mathematical modeling of formation damage due to invasion of solid suspensions. *SPE Annual Technical Conference and Exhibition*, Houston, TX, October 2−5, 1988; SPE 18203.
(14) Kocabas, I.; Islam, M. R.; Modarress, H. *J. Pet. Sci. Eng.* **2000**, *26*, 19−30.
(15) Wang, S.; Civan, F. Productivity decline of vertical and horizontal wells by asphaltene deposition in petroleum reservoirs. *SPE International Symposium on Oilfield Chemistry*, Houston, TX, February 13−16, 2001; SPE 64991.
(16) Almehaideb, R. A. *J. Pet. Sci. Eng.* **2004**, *42*, 157−170.
(17) Monteagudo, J. E. P.; Rajagopal, K.; Lage, P. L. C. *Chem. Eng. Sci.* **2002**, *57*, 323−337.
(18) Dubey, S. T.; Waxman, M. H. *SPE Reservoir Eng.* **1989**, *6*, 389−395.
(19) Murgich, J. *Pet. Sci. Technol.* **2002**, *20*, 983−997.
(20) Moschopedis, S. E.; Fryer, J. F.; Speight, J. G. *Fuel* **1976**, *55*, 227−232.
(21) Soulgani, B. S.; Tohidi, B.; Jamialahmadi, M.; Rashtchian, D. *Energy Fuels* **2011**, *25*, 753−761.
(22) Lawal, K.; A.; Vesovic, V.; Boek, E. S. *Energy Fuels* **2011**, *25*, 5647−5659.
(23) *Annual Book of ASTM Standards*; American Society for Testing and Materials: Philadelphia, PA, 2005; Vol. *05.01*, Standard No. D2007-03.
(24) *Annual Book of ASTM Standards*; American Society for Testing and Materials: Philadelphia, PA, 2007; Vol. *05.01*, Standard No. D2172.
(25) *Annual Book of ASTM Standards*; American Society for Testing and Materials: Philadelphia, PA, 2007; Vol. *05.01*, Standard No. D3279.
(26) AlAwadhy, F.; Abou-Kassem, J. H.; Islam, M. R. Experimental and Numerical Modeling of Sulfur Plugging in a Carbonate Reservoir. *SPE International Petroleum Exhibition and Conference*, Abu Dhabi, UAE, October 11−14, 1998; SPE 49498.

(27) Zhu, B.-Y.; Gu, T. *Colloids Surf.* **1990**, *46*, 339−345.
(28) Ring, J. N.; Wattenbarger, R. A.; Keating, J. F.; Peddibhotla, S. *SPE Production Facil.* **1994**, *9*, 36−42.
(29) Flory, P. J. *J. Chem. Phys.* **1941**, *9*, 660.
(30) Jafari Behbahani, T.; Ghotbi, C.; Taghikhani, V.; Shahrabadi, A. *Sci. Iran. C* **2011**, *18* (6), 1384−1390.
(31) Xing, C.; Hilts, R. W.; Shaw, J. M. *Energy Fuels* **2010**, *24* (4), 2500−2513.
(32) Jafari Behbahani, T.; Ghotbi, C.; Taghikhani, V.; Shahrabadi, A. Experimental Study and Mathematical Modeling of Asphaltene Deposition mechanism in Core Samples. *Rev. Inst. Fr. Pet.* **2012**, submitted for publication.
(33) Jafari Behbahani, T.; Ghotbi, C.; Taghikhani, V.; Shahrabadi, A. *Energy Fuels* **2012**, *26*, 5080−5091.
(34) Jafari Behbahani, T.; Ghotbi, C.; Taghikhani, V.; Shahrabadi, A. Investigation of Asphaltene Deposition Mechanisms During Primary Depletion and CO_2 Injection. *9th European Formation Damage Conference*, Noordwijk, The Netherlands, June 7−10, 2011; SPE 143374.
(35) Coats, K. H.; Smith, B. D. *SPE J.* **1964**, *4*, 73−84.
(36) Bok, E.; Fadili, A.; Williams, M. J.; Padding, J. Prediction of Asphaltene Deposition in Porous Media by Systematic Upscaling from a Colloidal Pore Scale Model to Deep Bed Filtration. *SPE International Petroleum Conference and Exhibition*, Colorado, USA, October 30−November 2, 2011; SPE 147539.